JOURNAL OF MATERIALS SCIENCE **33** (1998) 5237–5241

Mechanical and thermal properties of Si–C–N material from polyvinylsilazane

T. NISHIMURA*, R. HAUG, J. BILL, G. THURN and F. ALDINGER
Max-Planck-Institut für Metallforschung, Pulvermetallurgisches Laboratorium, Heisenbergstrasse 5, D-70569 Stuttgart, Germany
E-mail: nishimur@nirim.go.jp

Commercial polyvinylsilazane was crosslinked and then crushed to powder. The powder was compacted by cold isostatic pressing at 630 MPa and pyrolysed at 1050 °C in flowing argon. Crack-free Si–C–N material was obtained. Bulk density of the material was 1.95 Mg m^{-3}. Open porosity was 9.6 %. The material was amorphous as a result of X-ray diffraction analysis. Elastic modulus measured by pulse–echo method was 105 GPa. Vicker's hardness calculated from indentation at 98 MPa was 6.1 GPa. Fracture toughness measured by indentation fracture method was 2.1 MPa $m^{1/2}$. Average bending strength was 118 MPa. The material shrank 1.9 % in length during heating up to 1400 °C in nitrogen. The thermal expansion coefficient of the material heat treated up to 1400 °C increase from 3.08×10^{-6} °C^{-1} at 100 °C to 3.96×10^{-6} °C^{-1} at 1200 °C.

1. Introduction

Silicon nitride and silicon carbide are candidates for high temperature structural materials since they have higher strength than metals and oxide ceramics at more than 1000 °C. Conventionally, these materials are fabricated by powder metallurgical method, which consists of powder mixing, forming of green bodies and sintering. They are typical covalent materials, therefore sintering of pure materials is difficult, because of low diffusion coefficients. In order to advance sintering, oxides and/or other impurities are added for assisting mass transport. During the cooling process, they form grain boundary phases and/or diffuse into the primary phase. Although such grain boundary phases are advantageous for the low temperature mechanical properties, at high temperature, the grain boundary phase becomes path of mass transport causing degradation of strength, creep and oxidation resistance [1].

One alternative route for the preparation of carbide- and nitride-based ceramics is the pyrolysis of preceramic polymers. In this connection, silicon carbide fibres were fabricated [2]. This technique can be applied for the fabrication of fibre-reinforced ceramic matrices composites [3] and for the preparation of heat and oxidation resistant coatings for C/C composites [4]. It has been difficult to fabricate dense bulk material by the method, because gaseous phase evaporates during pyrolysis and causes pores and cracks. Riedel *et al*. [5] fabricated Si–C–N and Si_3N_4 ceramics from polyhydridomethylsilazane with a residual open porosity of 7%. After cross-linking, the polyhydridomethylsilazane was milled, sieved, and compacted by cold isostatic pressing. Subsequent pyrolysis at 1000 °C in argon or ammonia atmosphere of the obtained green body yielded ceramic monoliths. $Si_{1.73}C_{1.0}N_{1.56}$ and Si_3N_4 materials could be made in argon and ammonia, respectively. Sintering additives are not necessary in the process. The materials fabricated by the method are highly heat resistant [6]. Vickers hardness of the material pyrolysed at 1150 °C was 10 GPa and bending strength was in the order of 170 MPa, respectively [7]. However, properties of bulk material from polyvinylsilazane and thermal properties of the polymer-derived Si–C–N materials have never been reported. In the present paper, bulk Si–C–N material is fabricated from polyvinylsilazane and mechanical and thermal properties are measured.

2. Experimental procedure

Commercial polyvinylsilazane (VT50, Hoechst AG, Germany) was heated at about 240 °C for 1 h in flowing argon and then for 1 h in vacuum. By the heat treatment, cross-linking occurred and solid polymer was obtained. The cross-linked polymer was crushed in a Teflon pot with zirconia balls by planetary mill. After the milling, the powder was sieved to remove agglomerates and large particles. The sieved powder was compacted by cold isostatic pressing at 630 MPa for 1 min. The dimension of the compacts was about $12 \times 20 \times 30$ mm. The compacts were pyrolysed at 1050 °C for 4 h in flowing argon. The heating rate was 100 °C h^{-1} up to 100 °C and 25 °C h^{-1} from 100 to 1050 °C. Cooling was done at the rate of 300 °C h^{-1}.

* Guest scientist from National Institute for Research in Inorganic Materials, Tsukuba, Japan.
Author for correspondence: Dr Toshiyuki Nishimura, National Institute for Research in Inorganic Materials, 1-1 Namiki, Tsukuba, Ibaraki 305-0044 Japan. E-mail: nishimur@nirim.go.jp.

For metallographic investigations, the specimens were polished and observed by an optical microscope (Model DAS, Leica, Bensheim, Germany). Bulk density, open porosity and pore size distribution were measured by mercury porosimetry (Porosimeter 2000, Carlo Erba Instruments, Milan, Italy). Crystallinity was measured by X-ray diffraction analysis (Difraktometer D5000, Siemens, Karlsruhe, Germany). Elastic modulus was determined by pulse-echo method. Vickers hardness was measured varying indentation loads from 0.98 to 98 N. For the indentation at 0.98–9.8 N, microhardness tester (Micromet 1, Buehler, Illinois, USA), for 9.8–98 N, Vicker's hardness tester (Model 1900, Buehler, Illinois, USA) were used. In measuring micro Vicker's hardness, care was taken to indent on pore-free area in order to obtain clear indents. More than five indentations were conducted at each load. Fracture toughness was measured by the indentation fracture method (designated IF method) as reported by Anstis *et al*. [8]. The indentation load was 98 N. The fracture toughness, K_{IC}, was calculated using Equation 1

$$K_{IC} = 0.016E^{1/2}H^{1/2}(P/c^{3/2}) \quad (1)$$

where E is Elastic modulus (GPa), H is Vicker's hardness (GPa), P is Indentation load (N), c is half length of median crack (m).

For strength measurements the Four-point bending apparatus was used. The rectangular specimens for bending were cut from the pyrolysed samples and polished. The dimension of the specimens were $3 \times 4 \times 25$ mm. The inner and outer span were 7 and 20 mm, respectively. The cross-head speed was 0.0083 mm s^{-1} (0.5 mm min^{-1}). For loading, a testing machine (Schenck, Hydropuls PSA2017, Darmstadt, Germany) was used.

The specimens for dilatometric measurements were produced by the same procedure as explained above. The dimension of cylindrical mould for cold isostatic pressing was 10 mm in diameter and 15 mm in length. After the pyrolysis, the dimension of specimens was about 6 mm in diameter and 9 mm in length. Thermal expansion behaviour of the pyrolysed specimens was measured up to 1400 °C in nitrogen using a dilatometer (Theta, NY, USA).

3. Results and discussions

3.1. Materials

After the pyrolysis at 1050 °C, crack-free, black and bulk bodies were obtained (Fig. 1). The dimension of the specimen in Fig. 1 was about $9 \times 15 \times 23$ mm. No cracks were observed on the surface. To obtain a small piece of specimen for the mercury porosimetry, the specimens were cut. Any cracks were not observed inside.

For microstructural evaluation, a polished surface of the specimen was observed by optical microscope (Fig. 2). White parts correspond to the solid phase and black parts to pores. Large pores with over ten micrometer in diameter were observed.

In order to evaluate a pore structure quantitatively, the pore size distribution of the material was measured by the mercury porosimeter. The bulk density, 1.95 Mg m^{-3}, was calculated from the mass and the volume of a specimen in mercury. The open porosity was 9.6% as calculated from the mass and mercury penetration volume after a penetration pressure of 200 MPa was applied. The pore size distribution is bimodal (Fig. 3). The larger and smaller mode is about 30 and 0.3 μm, respectively. The larger mode supposed to come from the large pores observed in Fig. 2. Although the number of the larger pores is small, they are critical for the strength.

As the X-ray diffraction analysis varying 20 from 10 to 80°, any peaks were not detected. This means that the material is amorphous. Chemical composition of the as-pyrolysed material was $Si_{1.0}C_{1.6}N_{1.3}$ [9]. Seitz *et al*. [10] reported that the ceramic contained a high amount of sp^2-carbon and SiN_4 tetrahedrons. Polyvinylsilazane contains [—SiVi$(NH)_{0.5}$NH—]-structural units and a small number of end group [—SiVi(NH)NMe_2—] (Me = CH_3, Vi = CH_2CH) [11].

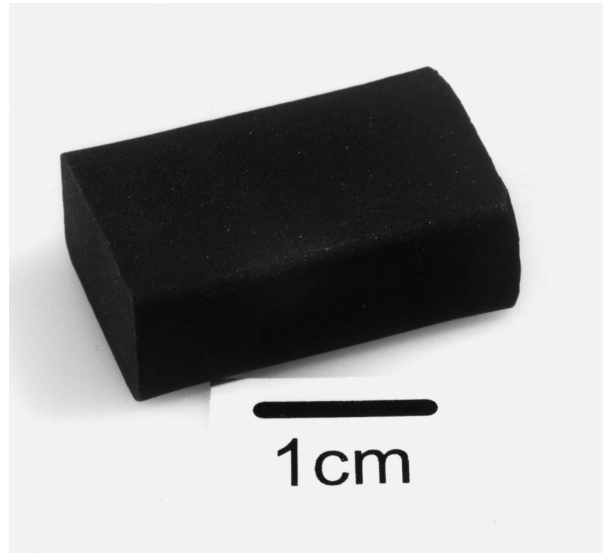

Figure 1 Appearance of a polyvinylsilazane-derived Si–C–N ceramic monolith.

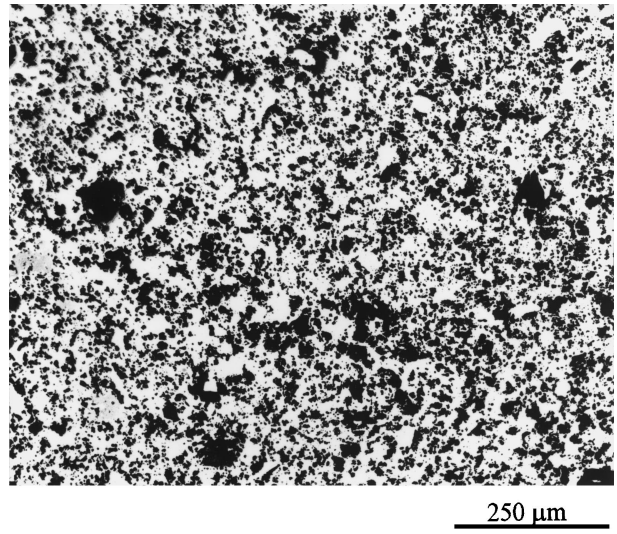

Figure 2 Optical micrograph of the polished surface of a polyvinylsilazane-derived Si–C–N ceremic monolith.

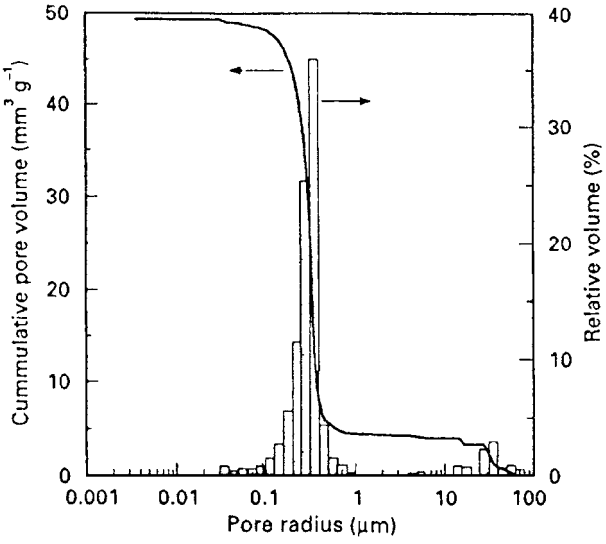

Figure 3 Pore size distribution of a polyvinylsilazane-derived Si–C–N ceramic monolith.

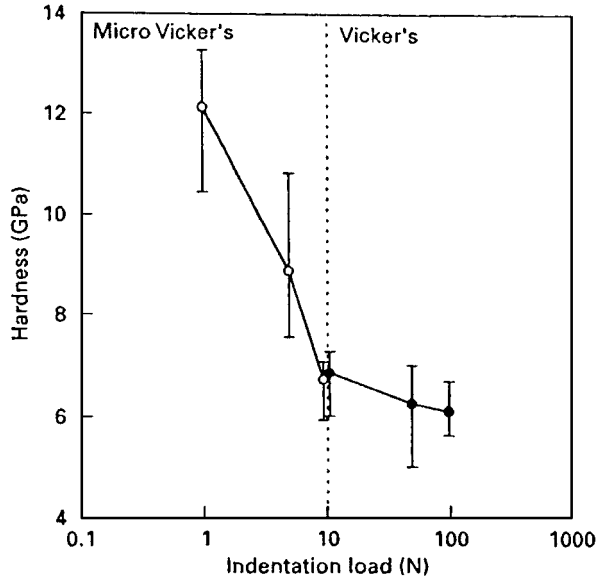

Figure 4 Dependence of Vickers hardness on indentation load.

The reactions during cross-linking and pyrolysis are not clearly understood, but Riedel *et al.* [7] suggested three requirements for crack-free polymer to ceramic transformation. The first is infusibility of cross-linked powder, second is presence of transient porosity and third is formation of covalent bonds between the individual powder particles. In the present work, a green body of cross-linked powder contains a number of interparticle pores, which provide paths for evaporation. And also the green body is compacted enough dense to form covalent bonds between the individual particles during pyrolysis. As shown in the Fig. 2, large pores still exist in the pyrolysed body. By optimizing the compaction process, denser pyrolysed bodies may possibly be obtained.

3.2. Mechanical properties

Elastic modulus measured by pulse-echo method is 105 GPa. That of silicon nitride and silicon carbide which are fabricated by the conventional method is about 300 and 410 GPa, respectively [1]. The primary reason for the low elastic modulus is the existence of pores. Though a number of equations on the relationship between elastic modulus and porosity have been proposed, in any equation, the elastic modulus of the porous material decreases with the increase of the porosity [12]. The elastic modulus of glass with 2% pore is 3.9% lower than that of pore-free glass [13]. Another reason is that the material is amorphous. The elastic modulus is closely related to the force between atoms and increases with the increase of the atomic force. As has been shown, the ceramic material obtained by pyrolysis of the polyvinylsilazane contained a high amount of SiN_4 tetrahedrons [10], but no long-range order. Therefore, average force between silicon and nitrogen atoms in amorphous is weaker than that in the crystalline phase.

Vickers hardness was measured varying the indentation loads. Average hardness of more than five indentations is plotted in Fig. 4. Upper and lower error bar of each plot means the maximum and minimum value, respectively. For indenting at lower loads (0.98–9.8 N) microhardness tester and for higher indentation loads (9.8–98 N) Vickers hardness tester were used. As the measured value with load of 9.8 N was the same with both techniques, differences in measured value between the two tester could be neglected. The Vickers hardness decreases drastically from 12.1 to 6.7 GPa with the increase of the indentation load from 0.98 to 9.8 N. At higher indentation loads, the hardness decreases gradually with the increase of the load. The average value of the hardness at 98 N is 6.1 GPa. The tendency that hardness at lower indentation loads is higher than that at higher loads is well known. Additionally, in the present work, the effect of the pores may not be neglected. The effect of pores is less at lower indentation loads, because the indentation was done selectively on pore-free areas. At higher loads, pores always exist in the indent, because the size of the indent is large as compared to the size and distance of pores. The Vickers hardness of Si–C–N materials from polyhydridomethylsilazane was 10 GPa. This material was fabricated at 1150 °C and the open porosity was 6% [7]. The present material could be densified even more because it shrank by heat treatment at higher 1050 °C as shown in the next section. The elastic modulus and Vickers hardness will increase with the densification by heat treatment at higher temperature.

Fracture toughness measured by indentation fracture method is 2.1 MPa $m^{1/2}$. The value is higher than that of oxide glasses but lower than that of polycrystalline silicon nitride or silicon carbide [8]. The reason for the low fracture toughness is that the material is amorphous. When a crack propagates in a pore, its propagation may be interrupted by stress release at the crack tip. This means a decrement of c in Equation 1 and an overestimation of K_{IC}. Because the present material contains 9.6% of porosity, the fracture toughness of pore-free material is probably lower than 2.1 MPa $m^{1/2}$.

The average bending strength of seven specimens is 118 MPa. The maximum and minimum values are

146 and 88 MPa, respectively. The bending strength of amorphous ceramic derived from polyhydridomethylsilazane fabricated 1150 °C was in the order of 170 MPa [7]. Because the open porosity of the material was less, this might be the primary reason for higher strength than that of the present material. Relationship between strength (σ_f), fracture toughness (K_{IC}) and crack size (c) is expressed by Equation 2

$$\sigma_f = \frac{1}{Y}\frac{K_{IC}}{c^{1/2}} \quad (2)$$

The Y is a constant which is related with shape of crack. Using Equation 2, 118 MPa for the strength, 2.1 MPa $m^{1/2}$ for K_{IC} and 1.174 for Y, crack size was estimated to be 230 μm. This value is much larger than the larger mode of pore radius, 30 μm and observed large pores by optical microscope. One of the possibility is that single pores of that size existed in the material. The possibility of the existence of such large pores cannot be denied because larger pores than 70 μm cannot be measured by the mercury porosimeter and the observed surface was a small part of the whole specimen. Another possibility is that pore agglomeration acts as a large fracture origin. In this case, it is difficult to correlate strength and pore size distribution. Pores, which are large enough to be a fracture origin, should be removed in order to improve the strength. Dense green compact with fine pores distributing homogeneously is desirable.

3.3. Thermal properties

In order to confirm thermal stability of the material, the cylindrical specimen was heated up to 1400 °C in nitrogen. The heating and cooling rate was both 10 °C min^{-1} (this heat treatment is designated HT1). For calculation of thermal expansion coefficient, the same sample was heated up to 1400 °C. In order to obtain the relationships between temperature and length more precisely, heating and cooling rate were decreased at 2 °C min^{-1} (designated HT2). Fig. 5 shows the length related to the original length of the specimen during HT1 and HT2. During HT1, the specimen expanded linearly up to 1000 °C and then shrank drastically at temperatures above 1100 °C. In the cooling procedure, the specimen shrank linearly at temperatures below 1200 °C. The amorphous ceramic pyrolysed at 1050 °C shrank by heat treatment above 1050 °C. Total shrinkage by HT1 was 1.9%. During HT2, the specimen expanded linearly up to 1200 °C and shrank above 1200 °C. This means that shrinkage at 1400 °C did not complete by HT1 and the ceramic was still unstable at 1400 °C. The shrinkage during cooling was linear below 1300 °C. Though total heating time of HT2 was longer than that of HT1, total shrinkage in HT2 was less than that in HT1. Because the specimen shrank at temperatures above 1200 °C during heating in HT2, which meant it was still unstable, the heat treatment for the calculation the thermal expansion coefficient was repeated. The heating and cooling rate was 2 and 3 °C min^{-1}, respectively (designated HT3). The shrinkage was linear until 1300 °C during heating. At

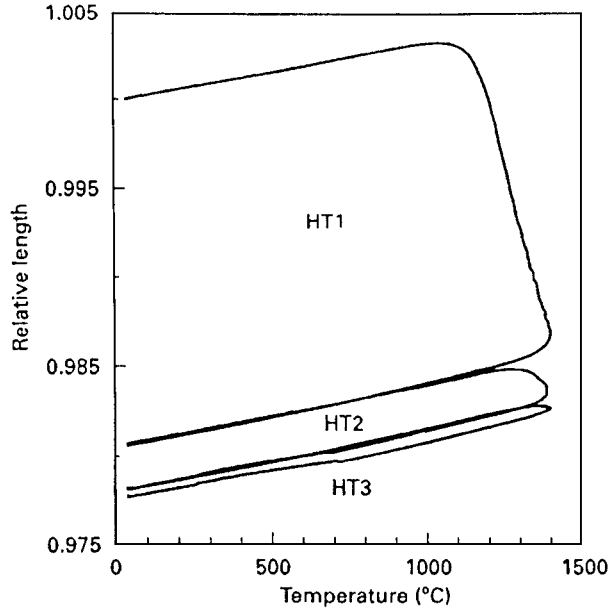

Heat treatment	Heating rate (°C min^{-1})	Cooling rate (°C min^{-1})
HT1	10	10
HT2	2	2
HT3	2	3

Figure 5 Shrinkage curve of a polyvinylsilazane-derived Si–C–N ceramic monolith during heat treatment up to 1400 °C in nitrogen.

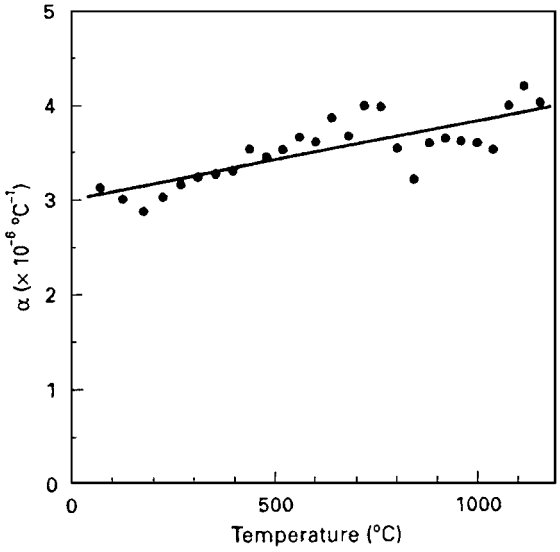

Figure 6 Thermal expansion coefficient, α, of a polyvinylsilazane-derived Si–C–N ceramic monolith heat treated up to 1400 °C.

temperatures above 1300 °C, shrinkage still occurred, but the amount of shrinkage was much less than that in HT2. During cooling, shrinkage was linear below 1300 °C. Non-linearity observed below 700 °C seemed to be an instrumental error. Comparing the shrinking behaviour during heating at HT2 and HT3, the starting temperature of shrinkage at HT3 was higher than that at HT2 and total shrinkage at HT3 was less than that at HT2. It seems to take a certain long time to complete the densification at 1400 °C. The $Si_{1.73}C_{1.0}N_{1.56}$ material fabricated at 1000 °C from polyhydridomethylsilazane shrank 3% in length by heat treatment at 1400 °C for 1 h in nitrogen [5]. The relative length of present material after HT3 is 0.978. Though the chemical composition

of the present material ($Si_{1.0}C_{1.6}N_{1.3}$) is different from the material from polyhydridomethylsilazane, apparent shrinkage is almost the same. Using the expansion data at HT3 from 40 to 1200 °C, the thermal expansion coefficient is calculated. The thermal expansion coefficient (α) at $(t_1 + t_2)/2$ [°C] was calculated by

$$\alpha = \frac{(l_2 - l_1)}{(t_2 - t_1)} \tag{3}$$

where t_1, t_2 (°C) are temperature, l_1, l_2 are relative lengths at t_1 and t_2. $(t_2 - t_1)$ was about 50 °C. The thermal expansion coefficient at each temperature is plotted with black circle in Fig. 6. Though the plots scatter, the thermal expansion coefficient increases with the increase of temperature. The solid line was calculated using the least square method. The thermal expansion coefficient of silicon nitride and silicon carbide is about 3×10^{-6} and $4 \times 10^{-6}\,°C^{-1}$ respectively [1]. The solid line lies within the range.

4. Conclusions

Crack-free Si–C–N amorphous material was fabricated from commercial polyvinylsilazane Elastic modulus, Vicker's hardness, fracture toughness and bending strength were measured. They are lower than those of conventional silicon nitride and silicon carbide. The primary reason for the low value is the existence of pores. Recently, a dense green body could be obtained by uniaxial pressing the cross-linked powder at 250 °C. During pressing and heating, the powder deforms plastically, therefore dense pyrolysed bodies were obtained [14]. Plasticity is one of the advantages of polymers. Taking advantage of the plasticity, a dense and complex-shaped green body can be formed and it will reduce grinding process after pyrolysis. The Si–C–N material pyrolysed at 1050 °C shrank by heat treatment up to 1400 °C in nitrogen. In order to complete the shrinkage at 1400 °C, a certain length of heating time is necessary. The thermal expansion coefficient increases with increase of temperature. The thermal expansion coefficient at 100 and 1200 °C is calculated as 3.08×10^{-6} and $3.96 \times 10^{-6}\,°C^{-1}$, respectively. These values are almost in the same level as that of polycrystalline silicon nitride and silicon carbide. The bulk shrinkage and thermal expansion coefficient have not been reported so far. These data will be useful for determination of fabrication process and designing of composites.

References

1. R. RAJ, *J. Amer. Ceram. Soc.* **76** (1993) 2147.
2. S. YAJIMA, J. HAYASHI, M. OMORI and K. OKAMURA, *Nature* **261** (1976) 683.
3. H. MOROZUMI, K. SATO, A. TEZUKA, H. KAYA and T. ISODA, *Ceram. Int.* **23** (1997) 179.
4. J. BILL and D. HEIMANN, *J. Eur. Ceram. Soc.* **16** (1996) 1115.
5. R. RIEDEL, G. PASSING, H. SCHÖNFELDER and R. J. BROOK, *Nature* **355** (1992) 714.
6. R. RIEDEL, H.-J. KLEEBE, H. SCHÖNFELDER and F. ALDINGER, *ibid.* **374** (1995) 526.
7. R. RIEDEL, M. SEHER, J. MAYER and D. V. SAZABO, *J. Eur. Ceram. Soc.* **15** (1995) 703.
8. G. R. ANSTIS, P. CHANTIKUL, B. R. LAWN and D. B. MARSHALL, *J. Amer. Ceram. Soc.* **64** (1981) 533.
9. J. SEITZ, PhD thesis, Universität Stuttgart (1996).
10. J. SEITZ, J. BILL, N. EGGER and F. ALDINGER, *J. Eur. Ceram. Soc.* **16** (1996) 885.
11. J. BILL, R. RIEDEL and F. ALDINGER, in Fourth Euro Ceramics vol. 4. Basic Sciences - Trends in Emerging Materials and Applications, edited by A. Bellosi, (Gruppo Editoriale Faenza Editrice S.p.A, Faenza, Italy, 1995) p. 125.
12. J. B. WACHTMAN, Jr, in National Bureau of Standards Special Publication 303, edited by J. B. Wachtman, Jr. (Washington, 1969) p. 139.
13. D. P. H. HASSELMAN and R. M. FULRATH, *J. Amer. Ceram. Soc.* **47** (1964) 52.
14. J. SEITZ and J. BILL, *J. Mater. Sci. Lett.* **15** (1996) 391.

Received 15 August 1997
and accepted 11 May 1998